Journal of Alloys and Compounds 509S (2011) S747–S749

Contents lists available at ScienceDirect

Journal of Alloys and Compounds

journal homepage: www.elsevier.com/locate/jallcom

Direct synthesis of sodium alanate with novel catalytic TiB_2

Li Li, Yijing Wang*, Yaping Wang, Guang Liu, Yan Han, Fangyuan Qiu, Chao Yan,
Dawei Song, Lifang Jiao, Huatang Yuan

Institute of New Energy Material Chemistry, Key Laboratory of Advanced Energy Materials Chemistry (MOE), Nankai University, Tianjin 300071, PR China

ARTICLE INFO

Article history:
Received 22 July 2010
Received in revised form
30 September 2010
Accepted 12 October 2010
Available online 23 October 2010

Keywords:
Metal hydrides
TiB_2
Hydrogen storage material
Catalysis

ABSTRACT

A novel catalyst TiB_2 is used in preparing TiB_2-doped sodium aluminium hydride under a low hydrogen pressure. $NaAlH_4$ can be directly synthesized by using TiB_2 as catalyst in about 5 h at 2 MPa hydrogen pressure. It shows that TiB_2 has a remarkable catalytic effect and can enhance the performance of hydrogen release. The highest hydrogen desorption capacity of the sample doped with 8 mol% TiB_2 is 5.02 wt.%. Thus, TiB_2 particles synthesized is a promising catalyst for synthesizing and catalysing the hydrogen absorption and desorption in light-metal complex hydrides.

1. Introduction

Owing to the limited supply of fossil fuels, hydrogen has attracted massive attention as an alternative energy carrier [1–5]. A key technical challenge for hydrogen application is how to develop a viable on-board storage medium. In the past few decades, lots of efforts have been made to explore on-board hydrogen storage systems, such as compressed hydrogen gas, cryogenic and liquid hydrogen, metal hydrides [6–14]. However, all of them lack efficiency for commercial applications. Recently, light metal complex hydrides are the focus of research for vehicular hydrogen storage. Among various metal complex hydrides [15–20], sodium aluminium hydride ($NaAlH_4$) is considered as one of the most suitable solid-state hydrogen storage materials since Bogdanović and Schwickardi [21] found that Ti-catalyzed $NaAlH_4$ exhibited reversible hydrogen storage together with enhanced kinetics.

Recently, great attention has been paid to prepare $NaAlH_4$ by milling NaH/Al with catalysts under hydrogen atmosphere, because this method could effectively reduce the cost and improve the hydrogen absorption and desorption of $NaAlH_4$. J.M. Bellosta von Colbe synthesized $NaAlH_4$ by milling NaH/Al with $TiCl_3$ under hydrogen atmosphere with an initial pressure of 83 bar [22]. Later, Bitter [23] reported the synergistic effect on dehydrogenation kinetics of $NaAlH_4$ with doping Ti-catalyst. They discovered that the kinetics of $NaAlH_4$ had been improved greatly with doping 2 mol% Ti-catalyst. Moreover, Xiao et al. [24] reported that it was possible to achieve direct synthesis of $NaAlH_4$ by milling NaH/Al with TiF_3 catalyst for 50 h at 25 bar hydrogen pressure during the in situ hydrogenation process. However, there are many problems about the synthesis of $NaAlH_4$ by milling the NaH/Al mixture: long time of milling, high hydrogen pressure and byproduct. Therefore, it is necessary to explore a novel catalyst on the direct synthesis of $NaAlH_4$ from NaH and Al.

In this paper, $NaAlH_4$ was synthesized by dry ball milling NaH/Al with novel TiB_2 catalyst under 1–2 MPa hydrogen pressure at ambient temperature. The hydrogen desorption performance of $NaAlH_4$ was also tested.

2. Experimental

2.1. Synthesis of $NaAlH_4$

The mixture of NaH(97%, Alfa Aesar)/Al(99.5%, Alfa Aesar) and 8 mol% TiB_2 (synthesized by solid state reaction) was introduced into a stainless steel vessel with stainless steel balls and milled in a planetary ball mill. The ball-to-powder weight ratio was 40:1, the mixture was milled (450 rpm) under Ar atmosphere for 15 h, and then milled (450 rpm) under 1–2 MPa hydrogen pressure for 0–40 h at ambient temperature. The different milling conditions of the samples are listed in Table 1. All the operations were carried out in the glove box (Super 1220/750/900) under purified argon atmosphere (H_2O: <10 ppm; O_2: <10 ppm).

2.2. Characterization

Phase compositions of the samples were studied by X-ray diffraction (XRD, Rigaku D/Max PC2500, Cu Kα radiation) and refined by GSAS program [25].

The dehydrogenation rates of the samples were measured at atmospheric pressure in flowing argon (about 35.3 ml/min) in a temperature programmed desorption (TPD, PX200) mode at a ramping rate of 2 °C/min. The weight loss percentage

---

* Corresponding author. Tel.: +86 22 23503639; fax: +86 22 23503639.
E-mail address: wangyj@nankai.edu.cn (Y. Wang).

0925-8388/$ – see front matter © 2010 Elsevier B.V. All rights reserved.
doi:10.1016/j.jallcom.2010.10.064

Table 1
Samples' preparation conditions.

Name	Milling time under Ar	Hydrogen pressure	Milling time under H2
S1[a]-5[b]	15 h	1 MPa	5 h
S1-10	15 h	1 MPa	10 h
S1-20	15 h	1 MPa	20 h
S1-30	15 h	1 MPa	30 h
S1-40	15 h	1 MPa	40 h
S2-0	15 h	2 MPa	0 h
S2-5	15 h	2 MPa	5 h
S2-10	15 h	2 MPa	10 h
S2-15	15 h	2 MPa	15 h

a: hydrogen pressure; b: milling time under H_2. (e.g.: S1[a]-5[b], the mixture was milled under Ar atmosphere for 15 h, and then milled under 1 MPa hydrogen pressure for 5 h at ambient temperature.)

of the samples was calculated according to the weight of $NaAlH_4$ in the reactor.

3. Results and discussion

3.1. Effect of milling time

Fig. 1 shows the X-ray diffraction patterns of as-prepared samples. Detailed preparation conditions for those samples are given in Table 1. As shown in Fig. 1a, the diffraction peaks of NaH and Al are broad and weak, and some peaks of Na_3AlH_6 appear in sample S1-5. In sample S1-10, Na_3AlH_6 becomes the main phase. When the milling time increases to 20 h (S1-20) and 30 h (S1-30), the peak intensity of Na_3AlH_6 gradually decreases and $NaAlH_4$ peaks become sharp. As the milling time increases to 40 h (S1-40), Na_3AlH_6 diffraction peaks completely disappear, suggesting that Na_3AlH_6 is completely hydrogenated to form $NaAlH_4$. In addition, when the hydrogen pressure is 2 MPa (Fig. 1b) without ball-milling (S2-0), no new phase appears. And when the ball-milling time is 5 h (S2-5), the diffraction peaks of NaH almost disappear and some peaks of $NaAlH_4$ and Na_3AlH_6 can be detected. This demonstrates that the hydrogenation reaction $NaAlH_4$ occurs in a relatively short ball milling time. The conversion of $NaAlH_4$ can be completed under the synthesis condition of sample S2-15, exhibiting a high kinetic of hydrogenation.

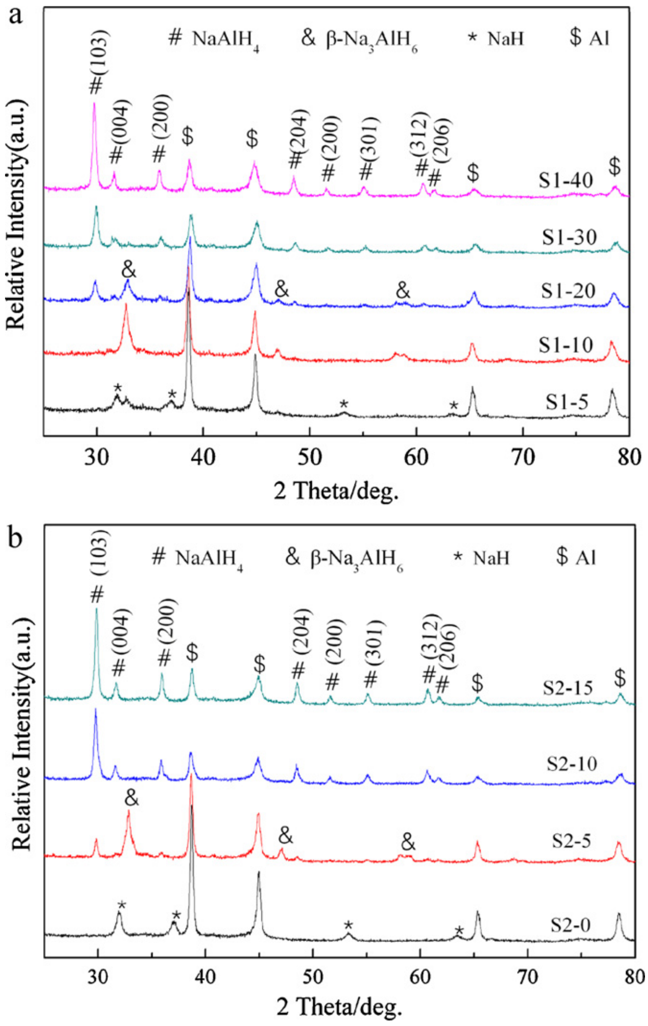

Fig. 1. X-ray diffraction patterns of all samples: (a) ball-milling under 1 MPa hydrogen pressure and (b) ball-milling under 2 MPa hydrogen pressure. Detailed preparation processes for those samples are given in Table 1.

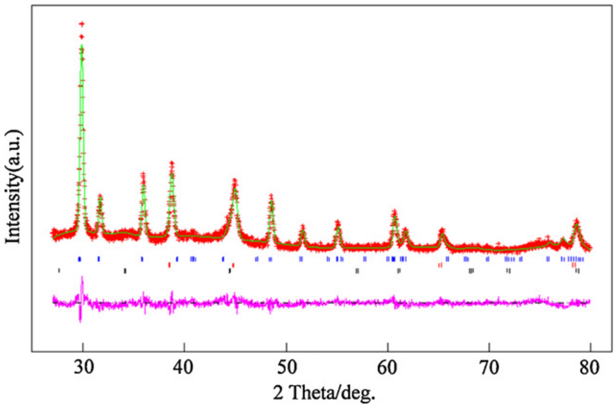

Fig. 2. GSAS refinement results of the sample S2-15. Vertical bars (from above) correspond to the position of Bragg peaks for $NaAlH_4$, Al and TiB_2, respectively (XRD, Cu Kα radiation, $\lambda = 1.54056$ Å).

GSAS refinement is used to analyse the phase composition of the S2-15 sample. The calculated curve agrees well with the observed XRD pattern as shown in Fig. 2. It can be seen that $NaAlH_4$, Al and TiB_2 phases are existed in the S2-15 sample. The GSAS refinement results shown in Table 2 show that the contents of the $NaAlH_4$, Al and TiB_2 phases are 57.53 wt.%, 23.90 wt.% and 18.57 wt.%, respectively.

3.2. Effect of hydrogen pressure

As shown in Fig. 1a, when the hydrogen pressure is 1MPa, the peaks of NaH and Al become broad and weak, and some peaks of Na_3AlH_6 appear in sample S1-5. And Na_3AlH_6 is the main phase in sample S1-10. When the hydrogen pressure increases to 2 MPa (Fig. 1b), the diffraction peaks of NaH in sampe S2-5 almost disappear and some peaks of $NaAlH_4$ and Na_3AlH_6 can be detected. And the diffraction peaks of Na_3AlH_6 almost disappear and $NaAlH_4$ is the dominant phase in sample S2-10. Therefore, a higher hydrogen pressure is helpful for the conversion of Na_3AlH_6 to $NaAlH_4$.

Moreover, variation of the relative abundance of the $NaAlH_4$, Na_3AlH_6, Al, TiB_2 of S1-10, S1-20, S1-30 and S1-40 samples from GSAS refinement results are shown in Fig. 3. It can be seen that the content of $NaAlH_4$ phase in sample S1-20 is about 11.20 wt.%, which

Table 2
GSAS refinement results of the S2-15 sample.

Sample	Phase	Phase content (wt.%)	Rehydrogenation capacity (wt.%)
S2-15	$NaAlH_4$	57.53	4.95
	Al	23.90	
	TiB_2	18.57	

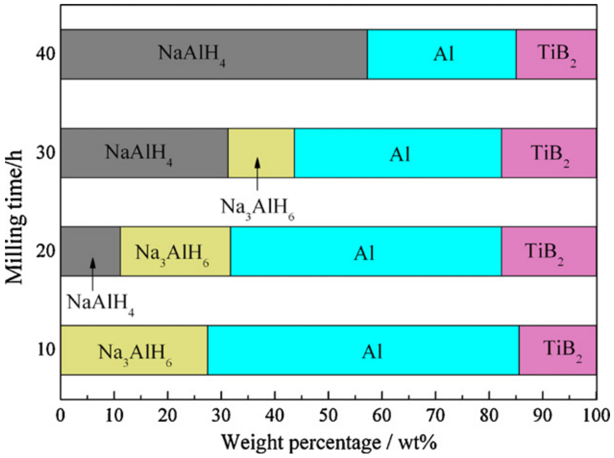

Fig. 3. Variation of the relative abundance of the $NaAlH_4$, Na_3AlH_6, Al, TiB_2 of S1-10, S1-20, S1-30 and S1-40 samples from GSAS refinement results.

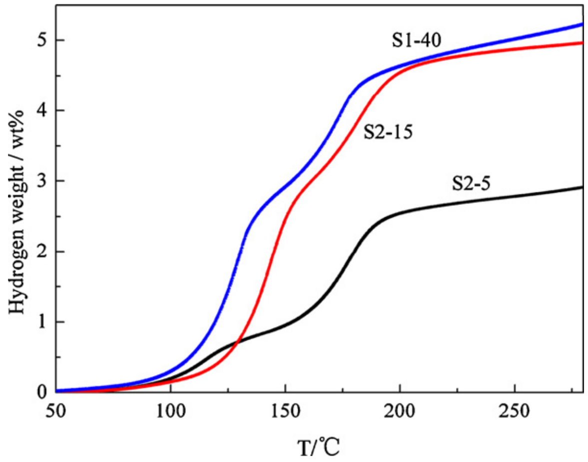

Fig. 4. TPD curves of the S2-5, S2-15 and S1-40 samples (the heating rate is 2 °C/min).

increases to 31.26 wt.% in sample S1-30 and 57.27 wt.% in sample S1-40. It can be concluded that the amount of $NaAlH_4$ increases with the milling time. In addition, the weight percentage of Na_3AlH_6 phase decreases gradually (27.44 wt.% in S1-10, 20.55 wt.% in S1-20, 12.39 wt.% in S1-30) and finally vanishes in S1-40 sample.

3.3. Thermal decomposition characteristics

Fig. 4 displays the hydrogen desorption of the S2-5, S2-15 and S1-40 samples. All the TPD curves exhibit two characteristic plateau regions. It is suggested that there are two weight loss steps which are attributed to the dehydrogenation of the synthesized $NaAlH_4$ and Na_3AlH_6, respectively. The TPD curve of the S2-5 system exhibits two weight-loss steps of 0.878% and 1.93 wt.%. And the two weight-loss steps of S2-15 sample obviously increase to 3.01% and 1.94 wt.%. It can be also seen obviously from Fig. 4 that the content of the $NaAlH_4$ phase increases with the milling time. In addition, the two weight-loss steps of S1-40 sample reach to about 3.12% and 1.90 wt.%. And the total dehydrogenation capacities observed are about 5.02 wt.%. These results show that TiB_2 plays an essential role in the synthesis and decomposition of $NaAlH_4$.

4. Conclusions

$NaAlH_4$ nanocrystalline is successfully obtained with TiB_2 catalyst via ball milling the mixture of commercial NaH and Al powder under hydrogen. With the increase of hydrogen pressure and milling time, the synthetic efficiency of $NaAlH_4$ increases significantly. And the highest dehydrogenation capacity observed is about 5.02 wt.%. It demonstrates that TiB_2 is a promising catalyst for enhancing hydrogen release in light-metal complex hydrides. Further investigations about the function of TiB_2 in the systhesis of sodium alanate hydride are on the way.

Acknowledgements

This work was financially supported by MOST projects (2007AA05Z149, 2007AA05Z108, 2010CB631303), NSFC (50631020, 50701025, 50971071 and 20873072) and MOE (IRT-0927).

References

[1] L. Schlapbach, A. Züttel, Nature 414 (2001) 353–358.
[2] W. Grochala, P.P. Edwards, Chem. Rev. 104 (2004) 1283–1315.
[3] P. Chen, Z.T. Xiong, W.Z. Luo, K. Lin, K.L. Tan, Nature 420 (2002) 302–304.
[4] K. Yvon, B. Bertheville, J. Alloys Compd. 425 (2006) 101–108.
[5] D. Chandra, J.J. Reilly, R. Chellappa, JOM 58 (2006) 26–32.
[6] H.W. Brinks, C.M. Jensen, S.S. Srinivasan, B.C. Hauback, D. Blanchard, K. Murphy, J. Alloys Compd. 376 (2004) 215–221.
[7] V. Ozolins, E.H. Majzoub, T.J. Udovic, J. Alloys Compd. 375 (2004) 1–10.
[8] S. Satyapal, J. Petrovic, C. Read, G. Thomas, G. Ordaz, Catal. Today 120 (2007) 246–256.
[9] L.C.J. Rowsell, O.M. Yaghi, J. Am. Chem. Soc. 128 (2006) 1304–1315.
[10] T. Ichikawa, S. Isobe, N. Hanada, H. Fujii, J. Alloys Compd. 365 (2004) 271–276.
[11] K.A. Lokshin, Y.S. Zhao, Appl. Phys. Lett. 88 (2006) 131909–131911.
[12] F. Fang, S.Y. Zheng, G.R. Chen, G. Sang, B. He, S.Q. Wei, D.L. Sun, Acta Mater. 57 (2009) 1959–1965.
[13] F.H. Wang, Y.F. Liu, M.X. Gao, K. Luo, H.G. Pan, Q.D. Wang, J. Phys. Chem. C 113 (2009) 7978–7984.
[14] S.Y. Zheng, F. Fang, J. Zhang, L.X. Sun, B. He, S.Q. Wei, G.R. Chen, D.L. Sun, J. Phys. Chem. C 111 (2007) 14021–14025.
[15] A. Züttle, P. Wenger, S. Rentsch, P. Sudan, Ph. Mauron, C. Emmenegger, J. Power Sources 118 (2003) 1–7.
[16] S.C. Amendola, S.L. Sharp-Goldman, M.S. Janjua, N.C. Spencer, M.T. Kelly, P.J. Petillo, M. Binder, Int. J. Hydrogen Energy 25 (2000) 969–975.
[17] I.E. Malka, T. Czujko, J. Bystrzycki, Int. J. Hydrogen Energy 35 (2010) 1706–1712.
[18] P. Wang, X.D. Kang, H.M. Cheng, Chem. Phys. Chem. 6 (2005) 2488–2491.
[19] J.F. Mao, Z. Wu, T.J. Chen, B.C. Weng, N.X. Xu, T.S. Huang, Z.P. Guo, H.K. Liu, D.M. Grant, G.S. Walker, X.B. Yu, J. Phys. Chem. C 111 (2007) 12495–12498.
[20] X.D. Kang, Z.Z. Fang, L.Y. Kong, H.M. Cheng, X.D. Yao, G.Q. Lu, P. Wang, Adv. Mater. 20 (2008) 2756–2759.
[21] B. Bogdanović, M. Schwickardi, J. Alloys Compd. 253 (1997) 1–9.
[22] J.M. Bellosta von Colbe, M. Felderhoff, B. Bogdanović, F. Schüth, C. Weidenthaler, Chem. Commun. 37 (2005) 4732–4734.
[23] C.P. Baldeĭ, B.P.C. Hereijgers, J.H. Bitter, K.P.D. Jong, J. Am. Chem. Soc. 130 (2008) 6761–6765.
[24] X.Z. Xiao, L.X. Chen, X.L. Fan, X.H. Wang, C.P. Chen, Y.Q. Lei, Q.D. Wang, Appl. Phys. Lett. 94 (2009) 041907–041909.
[25] B.H. Toby, J. Appl. Cryst. 34 (2001) 210–213.